



ORIGINAL ARTICLE

Assessment of the effect of silica calcium phosphate nanocomposite on mesenchymal stromal cell differentiation and bone regeneration in critical size defect



Shams Altwaim^{a,*}, Mohammed Al-Kindi^a, Nihal AlMuraikhi^b, Sarah BinHamdan^c, Ahmad Al-Zahrani^a

^a Department of Oral and Maxillofacial Surgery, College of Dentistry, King Saud University, Riyadh, Saudi Arabia

^b Stem Cell Unit, Department of Anatomy, College of Medicine, King Saud University, Riyadh, Saudi Arabia

^c College of Medicine, Al-Faisal University, Riyadh, Saudi Arabia

Received 10 February 2021; revised 8 March 2021; accepted 9 March 2021

Available online 1 April 2021

KEYWORDS

Bone;
Regeneration;
Cell ceramic;
Craniofacial;
Reconstruction

Abstract Objective: The research was designed to assess silica calcium phosphate nanocomposite (SCPC) biocompatibility and bioactivity as an osteoinductive scaffold and cell carrier. Consequently, the ability of cell seeded SCPC implant to regenerate a critical size defect in rat calvarium.

Materials and Methods: The study was conducted in two parts. A series of in vitro experiments on bone marrow stromal cells (MSCs) seeded in the SCPC scaffold evaluated cell attachment, proliferation and osteogenic differentiation. In the second part, a cell seeded SCPC construct was implanted in rat calvarium and bone regeneration was assessed by histological examination to evaluate the newly formed bone quality and the residual graft volume.

Results: In vitro experimentation revealed that MSCs cultured on SCPC maintained viability and proliferation when seeded into the SCPC. Scanning electron microscopy demonstrated cell adhesion and calcium appetite formation, MSCs differentiated towards the osteogenic lineage as indicated by the upregulation of RUNX2, ALP, Col1a1 markers. Histological examination showed regeneration from the periphery and core of the defect with new bone formation at different stages of maturation.

* Corresponding author at: Ministry of Health, Riyadh, Saudi Arabia.

E-mail addresses: 436203341@student.ksu.edu.sa (S. Altwaim), mAlKindi@ksu.edu.sa (M. Al-Kindi), nalmuraikhi@ksu.edu.sa (N. AlMuraikhi), azahran@KSU.EDU.SA (A. Al-Zahrani).

Peer review under responsibility of King Saud University.



Conclusion: Regenerative medicine delivers promising solutions and technologies for application in craniofacial reconstruction. SCPC scaffold has the potential to be used as a cell carrier to achieve stem cell-based bone regeneration, which provides a viable alternative for treatment of challenging critical size defect.

© 2021 The Authors. Production and hosting by Elsevier B.V. on behalf of King Saud University. This is an open access article under the CC BY-NC-ND license (<http://creativecommons.org/licenses/by-nc-nd/4.0/>).

1. Introduction

Repair or augmentation of bone may be required following trauma, pathology, or congenital anomaly to restore bone volume and contour. Autogenous bone has long been considered the gold standard for bone grafting, but it carries its own limitations, such as infection, resorption, scarcity, and donor site morbidity (Wan et al., 2006). Alloplastic bioactive ceramics are synthetic, chemically derived bone substitutes with rapidly advancing developments in manufacturing, contributing to its favorability. Alloplastic grafts structurally resemble the inorganic mineral phase of bone, making it a superior osteoconductive material and providing a template for cell attachment and guiding bone growth on its surface (Ducheyne and Qiu, 1999). However, a major drawback is the lack of a cellular component that would provide a source for bone progenitor cells to form new bone and resorb graft particles.

Cell-based bone engineering approaches encompass the sciences of materials, cell biology, and biotechnology to regenerate biological tissues (Meijer et al., 2007; Tang et al., 2016). Cell therapy requires the presence of an optimal environment to leverage cell function and direct cell differentiation to achieve maximum healing capacity. Bioactive ceramics, such as bioactive glasses, are candidate cell carriers owing to their unique biomimetic structure and dynamic ion dissolution (Will et al., 2012). The mineral composition of bioactive ceramics, mainly calcium phosphates, has been shown to induce stem cell differentiation toward the osteogenic lineage (Müller et al., 2008).

Recently, silica–calcium phosphate nanocomposite (SCPC) has been introduced as a promising silica-based scaffold with favorable bioactivity for applications in tissue engineering (El-Ghannam et al., 1999). The porous scaffold offers a high surface area for serum protein adsorption, cell attachment, and bone matrix development. The biomimetic features of the material result from ion dissolution and preferential precipitation, which enhance the bioactivity and rapid resorption of graft particles (El-Ghannam, 2005).

The critical size defect model is useful for investigating challenging clinical scenarios that result from congenital deformity, trauma or pathology. A full thickness 8 mm defect in the cranium is considered critical, as it will not heal completely during an animal's lifespan (Spicer et al., 2012; Vajgel et al., 2014). The present research aims to investigate SCPC scaffold biocompatibility, bioactivity, and osteogenic effects on cultured bone marrow stromal cells. In addition, the study examines the ability of cell seeded SCPC construct to regenerate an 8 mm critical size defect in rat calvarium.

2. Materials and methods

2.1. Ethical approval

The Institutional Research Ethics Board of King Saud University College of Medicine approved the study. The experiments took place at Prince Naif Bin Abdulaziz Health Research Center in Saudi Arabia.

2.2. *In vitro*

2.2.1. Scaffold preparation

Silica–calcium phosphate nanocomposite (SCPC50®, Shefabone, USA) is a bioactive ceramic distinguished by its porous structure. To ensure sterility, the disks were immersed in 70% ethanol for 20 min, washed in phosphate buffered saline (PBS), and then dried under ultraviolet light for 1 h.

2.2.2. Cell culture and seeding

A cell line model developed for human bone marrow skeletal mesenchymal cells (MSCs) was employed in this study for *in vitro* experimentation (Simonsen et al., 2002). The cells were maintained in a basal culture medium comprised of DMEM, supplemented with 4 mM L-glutamine, 4500 mg/l D-glucose, 10% sodium pyruvate, 10% fetal bovine serum, 1% penicillin–streptomycin, and 1% nonessential amino acids (all reagents were purchased from Gibco-Invitrogen, USA). The cells were incubated in 5% CO₂ at 37 °C and 95% humidity. The cells were added dropwise on the prewetted disk's surface at a density of 6×10^4 cells per disk.

2.2.3. Cell morphology and attachment assessment

Scanning electron microscopy (SEM) was used to assess seeded cell morphology and adhesion. After 3 days of incubation, the cell seeded scaffold was washed with PBS and fixed in 2.5% glutaraldehyde (Sigma-Aldrich, USA). Sample processing started with 1% osmium tetroxide treatment for one hour, followed by serial dehydration and then gold coating. The samples were visualized using the Carl Zeiss Sigma VP Oxford Microanalysis S800.

2.2.4. Cell viability and proliferation assessment

To evaluate the biocompatibility and viability of MSCs loaded on SCPC, the Alamar Blue cell viability and proliferation assay was used according to the manufacturer's recommendations (Thermo Fisher Scientific) after incubation for three, five, and seven days. The resazurin reduction fluorescence was measured using a BioTek Synergy II microplate reader (BioTek Inc., Winooski, VT, USA).

For the LIVE/DEAD cell viability assay, the cell seeded scaffold was stained with ethidium homodimer and acridine orange. The samples were incubated in the dark for 5–10 min, washed with PBS to remove excess stain, and then examined under a fluorescent microscope.

2.2.5. Quantitative reverse transcription-polymerase chain reaction (qRT-PCR)

The gene expression profiles of specific osteogenic genes (Table 1) of cells seeded in the SCPC scaffold were analyzed after 14 and 21 days. The total RNA was extracted from the cell pallets using the RNAase extraction kit (Analytik Jena AG, Germany). Gene expression was determined by measuring the mRNA level from the cDNA with qRT-PCR done with fast SYBR Green using the Applied Biosystems ViiA™ seven Real-Time PCR System (Thermo Fisher Scientific Life Sciences). Following normalization to the reference gene GAPDH, the quantification of gene expression was carried out using the $2\Delta\Delta CT$ value method (Livak and Schmittgen, 2001).

2.3. In vivo

2.3.1. Primary cell isolation

Rat bone marrow stromal cells were isolated and cultured, as reported previously (Maniatopoulos et al., 1988). Briefly, the lower limbs of six-week-old Sprague-Dawley rats were harvested, and the bone marrow was flushed out with culture media. The media were collected and incubated in 5% CO₂ and 95% air at 37 °C. The cells were monitored and showed a predominantly classical fibroblast-like morphology. After further expansion, the second passage cells were seeded at 1×10^6 density and incubated for 24 h in preparation for in vivo implantation.

2.3.2. Surgical procedure

Sprague Dawley rats (250–300 g) were allowed to acclimate, while water and a standard laboratory diet were available ad libitum. General anesthesia was induced and maintained with ketamine and xylazine. Skin incision was created along the midline, the periosteum was sacrificed, and the calvarial parietal bone was exposed. A circular bicortical defect was created using a low-speed trephine bur. The defect measured 8 mm in

diameter and approximately 1.5 mm in depth. The craniotomy defect was filled with a SCPC disk alone (N = 10) or a cell seeded SCPC construct (N = 10) (Fig. 1). The skin was closed with Vicryl sutures, and the animals were resumed routine care and provided analgesics as needed.

2.3.3. Euthanasia

The animals were euthanized eight weeks after craniotomy using an anesthetic overdose. Tissue samples were removed en bloc using a cutting wheel and preserved in formalin.

2.3.4. Histological processing

The fixed samples were placed in formic acid for decalcification, dehydrated, sectioned along different depths of the defect, and then imbedded in paraffin wax. The cut sections were stained with hematoxylin and eosin and inspected under light microscopy for qualitative assessment of the newly formed bone.

3. Results

3.1. Scaffold characterization

The surface topography, bioactivity, and MSC attachment of the SCPC scaffold were assessed by SEM. The SCPC granules demonstrated a porous morphology with a well-ordered and uniform pore channel structure, and cells were found filling the pores. Higher magnification showed that the cells extended over the pore opening with pseudopodia cytoplasmic extensions to anchor the cells to the surface. MSCs cultured in osteoblast induction media had attached, flattened, and spread across the calcium phosphate layer, which formed over the scaffold surface. Moreover, there were clusters of spherical-shaped apatite crystals of varying sizes (Fig. 2).

3.1.1. Cell function and scaffold compatibility

The viability and proliferation of MSCs cultured on SCPC scaffolds was assessed after 3, 5, and 7 days of incubation using the Alamar Blue assay. Although cells cultured on the SCPC scaffold showed lower proliferation compared to the control cells, they had a positive trajectory, with an increased proliferation rate over time (Fig. 3).

After 3 days of incubation, a LIVE/DEAD assay revealed cells with intact cell membranes (green) attached to the SCPC scaffold. A negligible number of dead cells (red) were observed, indicating near-complete viability. Higher magnification showed the characteristic spindle shape of the stromal cells and the brightly colored nucleus (Fig. 3).

3.1.2. Expression of osteogenic genes

The expression of osteoblast-related genes was measured for cells cultured on SCPC scaffolds after 14 and 21 days. The overall expression was higher for cells grown on SCPC, while the control cells maintained a constant level of expression after 14 and 21 days. On day 14, OSP, Runx, and ALP were upregulated, while OSC and collagen I were downregulated. ALP had the highest expression, although it declined thereafter. Gene expression on day 21 demonstrated upregulation of collagen I, RNX2 and osteopontin. Remarkably, the expression of the Colla1 gene increased dramatically over time to reach ninefold (Fig. 4).

Table 1 Characteristics of the primers used in the study.

Gene	Primer sequence (forward/reverse)
RUNX2	Forward: CACCATGTCAGCAAACTTCTT Reverse: ACCTTTGCTGGACTCTGCAC
ALP	Forward: GACGGACCCTCGCCAGTGCT Reverse: AATCGACGTGGGTGGGAGGGG
OSC	Forward: GGCAGCGAGGTAGTGAAGAG Reverse: CTCACACACCTCCCTCCTG
OSP	Forward: CAGTTCAGAAGAGGAGG Reverse: TCAGCCTCAGAGTCTTCATC
Collagen I	Forward: GAGTGCTGTCCCCTCTGCTG Reverse: TTTCTTGGTCCGGTGGGTG3
GAPDH	Forward: CTGGTAAAGTGGATATTGTTGCCAT Reverse: TGAATCATATTGGAACATGTAAACC

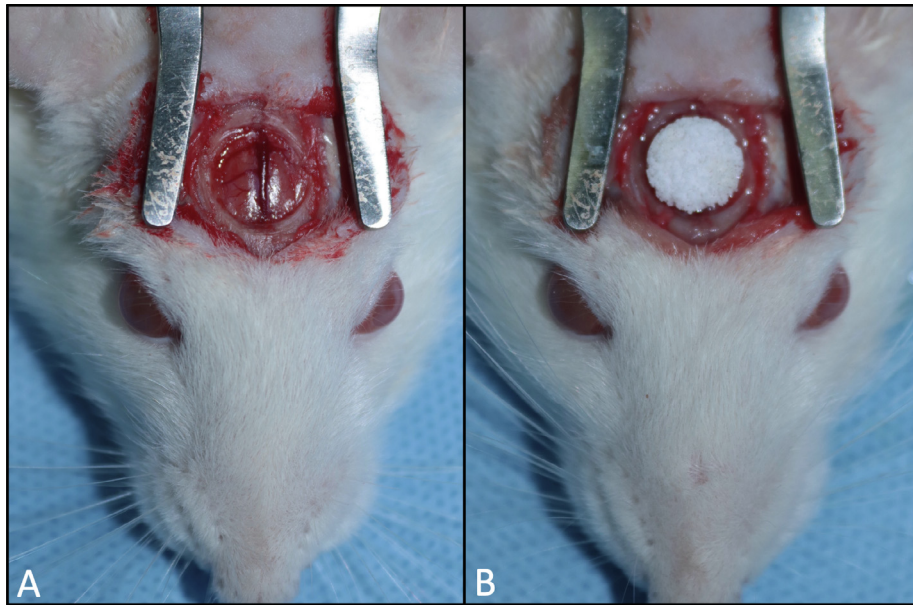


Fig. 1 Animal surgery (A) Full thickness defect in Rat calvarium exposing the dura. (B) Cell seeded SCPC construct implanted in the defect.

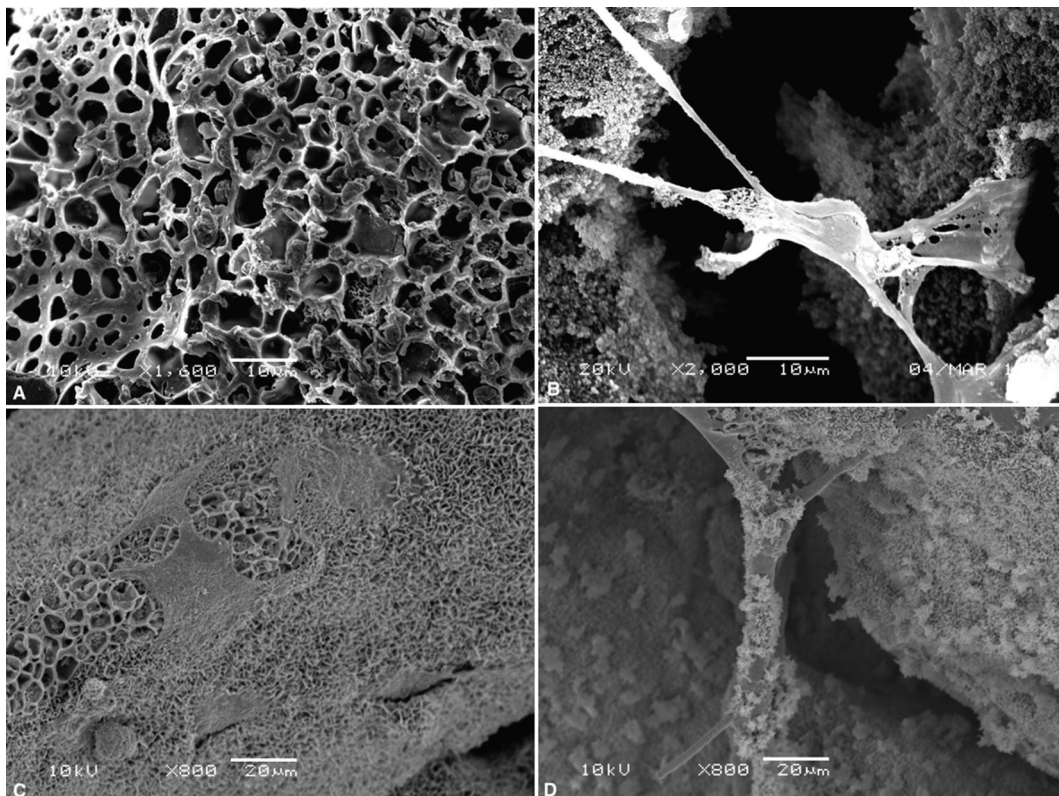


Fig. 2 SEM of SCPC scaffold (A) The porous morphology of the SCPC scaffold granules. (B) Cell extended over the pore opening with pseudopodia to anchor the cell to the surface. (C) Calcium phosphate layer formed over the scaffold surface and polygonal shaped cells in contact. (D) Deposition of spherical-shaped apatite.

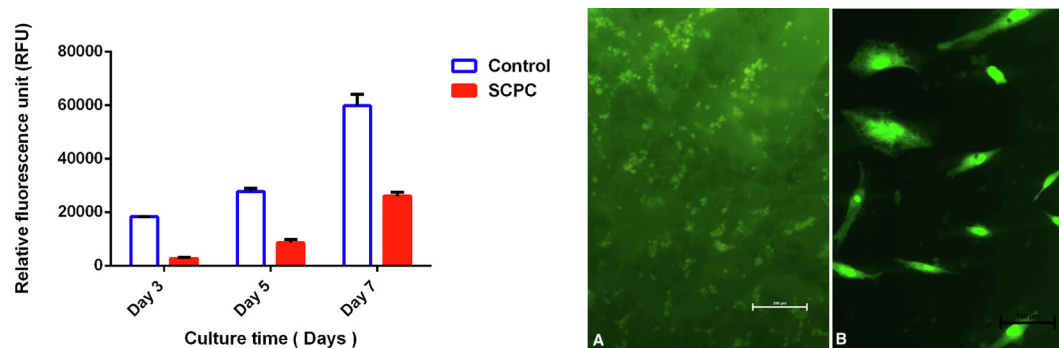


Fig. 3 The graph showing AlamarBlue® proliferation assay of cells cultured on SCPC. (A, B) Fluorescent images of cells grown on SCPC with intact membrane and brightly colored nucleus.

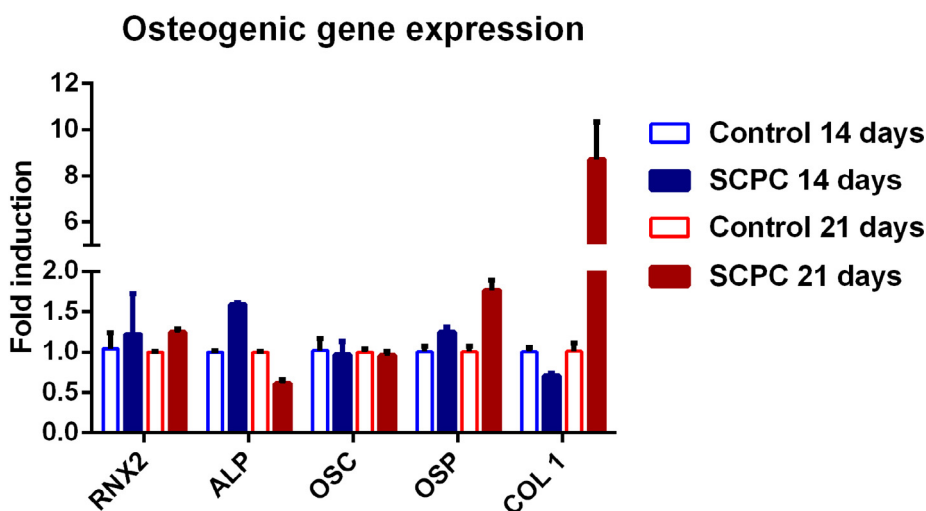


Fig. 4 Osteogenic gene expression analysis of cells grown on SCPC scaffold for 14 and 21 days in osteogenic media using quantitative real-time PCR.

3.2. In vivo

3.2.1. Histological analysis

Clinical examination of the harvested specimen showed that the SCPC implant was maintained in place and merged with the native bone at the edge of the defect.

The histological examination showed well-organized fibrous connective tissue infiltrating the graft and regeneration of the experimental defect with new bone formation in both groups. The regeneration was pronounced at the periphery of the defect, in addition to scattered islands of trabecular bone found in the center with interspersed residual graft particles. The newly formed bone at the periphery was more mature trabecular and woven bone and distinguished from the pre-existent cranial bone, which was lamellar and meagerly cellular. Towards the center, the bone islands consisted of woven bone and osteoid tissue. The remaining graft particles were surrounded by mild inflammatory infiltrates, with osteoclast-like cells on the surface. The experimental group treated with the cell seeded SCPC scaffold showed remarkably more mature newly formed bone, homogenous well-organized connective tissue fibers, and less residual graft material (Fig. 5).

4. Discussion

The field of tissue engineering has leaped through advances and discoveries in promising novel therapies, especially concerning bone tissue regeneration. In order for multipotent cells to attain their maximum healing capacity, the presence of the appropriate scaffold is mandatory to maintain cell viability and induce osteogenic differentiation. A promising bioactive ceramic with a characteristic chemical composition and porous structure has been proposed as a cell carrier for bone tissue engineering. The porous structure of SCPC provides a higher surface area for cell adhesion and vascular invasion and a template for bone formation, which will eventually expedite graft resorption (Liu and Ei-Ghannam, 2010). The graft interaction with biologic fluids primes dissolution kinetics and leads to the formation of the calcium phosphate appetite layer (El-Ghannam and Ning, 2006). The effect of the material composition and nanostructure was clearly demonstrated by SEM examination, showing the formation of the calcium phosphate layer, which acts as a platform for the precipitation of calcified apatite and cell adhesion mediated by the selective adsorption of fibronectin (Aniket et al., 2015). Gupta et al. (2007) found

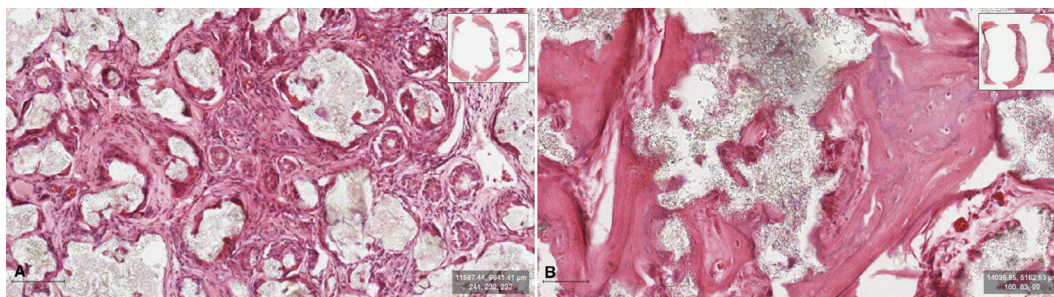


Fig. 5 Photomicrography of the decalcified section stain with H&E showing newly formed bone at different stages of maturation. (A) Experimental group grafted with SCPC disc only. (B) Experimental group grafted with cell seeded SCPC construct.

that the dissolution rate and the formation of a biological layer on the SCPC surface were significantly greater than those of bioactive glass.

The silica content of the material is essential for mimicking the inorganic phase of bone and enhancing bone remodeling via osteoinduction (Porter et al., 2004). Silicate ions encourage osteogenic differentiation of MSCs through the activation of the Wnt pathway, leading to widespread changes in the transcriptome profile and amplifying the expression of the bone-related genes OSC, OSP, and ALP (Carrow et al., 2018; Han et al., 2013). Silica has a strong stimulatory effect on *Colla1* expression by the preosteoblasts signal-regulated kinase pathway to produce collagen, which is an important component of the organic extracellular matrix (Mao et al., 2017; Reffitt et al., 2003; Shie et al., 2011). In our study, the remarkable upregulation of *Colla1* expression at 21 days is in line with the data reported by Gupta et al., who performed qRT-PCR analysis and showed the expression of OSP, OSC, and significant upregulation of *Colla1* in rat calvarial osteoblasts attached to SCPC compared to hydroxyapatite, tricalcium phosphate, or SCPC, with less silica content (Gupta et al., 2010, 2007). SCPC has an osteostimulatory effect that guides stromal cell differentiation, as established by the qRT-PCR results. Cells cultured on SCPC had increased expression of *RUNX2*, which is considered the orchestrator of osteoblastogenesis at all stages of development and maturation, by regulating osteoblast-related genes (Stein et al., 2004). The expression of osteopontin, which is found in osteoblasts, osteocytes, and osteoclasts, was maintained until day 21, indicating ongoing bone remodeling activity (Merry et al., 1993). Furthermore, ALP which initiates the mineralization process of the extracellular matrix, was upregulated on day 14 but declined thereafter (Rodrigues et al., 2016). These results are in accordance with the findings of Aniket, who found a similar pattern of ALP expression on day 14 (Aniket et al., 2015).

The results of the present study highlight the bone regeneration capacity of bone marrow stem cells when an appropriate microenvironment is created by a bioactive ceramic scaffold, such as SCPC. The experimental calvarial defect filled with cell seeded SCPC showed new bone formation at different stages of maturation, which demonstrates its ability for bone regeneration in a critical size defect. The challenge in the critical size defect is caused by the restricted migration or proliferation of the cells from the margins of the defect. The transplantation of stem cells provides a source for osteoblasts and overcomes host limitations, especially in older individuals where regenerative capacity is limited. Interestingly, in the cell seeded SCPC

implant group, new bone formation was noted at the center of the defect, indicating the osteoconduction and osteostimulatory effects of SCPC. In a study by Cardoso et al. (2007), the rat calvarial defect filled with blood clot or bioactive ceramics in the form of Biogran® and Perioglas® showed no statistical difference in newly formed bone volume up to 60 days. It was speculated that limited native stem cells and prolonged resorption of bioactive glass hindered the healing process. These findings are in accordance with the data presented by El-Rashidy et al. (2017), which demonstrated that the in vivo performance of bioactive glass was governed by the material's composition, fabrication method, and the 3D scaffold fabrication technique.

The porous structure of the SCPC scaffold overcomes the traditional disadvantages of bioactive glass by improving biodegradability and expedite bone regeneration. This study delivers the basis for the osteoinductive potential of the SCPC graft, which was demonstrated by the defect regeneration and filling with newly formed bone that was observed in the periphery and core of the defect. Future studies should consider the recruitment of larger animals and surgical sites with physiological loading to assess the materials' performance under functional stresses. Extending the study's time span will help us understand the ultimate fate of the material.

5. Conclusion

Regenerative medicine delivers promising technologies for application in craniofacial reconstruction. Bone tissue engineering using SCPC as a stem cell carrier is a promising approach owing to its superior biocompatibility, osteoinduction, and dissolution kinetics. The study adds to the mounting evidence supporting the use of bioactive ceramics and expands on its biological properties.

Declaration of Competing Interest

The authors declare that they have no known competing financial interests or personal relationships that could have appeared to influence the work reported in this paper.

Acknowledgement

The authors would like to thank Deanship of scientific research in King Saud University for funding and supporting this research through the initiative of DSR Graduate Students Research Support (GSR).

References

- Aniket, Reid, R., Hall, B., Marriott, I., El-Ghannam, A., 2015. Early osteoblast responses to orthopedic implants: synergy of surface roughness and chemistry of bioactive ceramic coating. *J. Biomed. Mater. Res. - Part A* 103, 1961–1973. <https://doi.org/10.1002/jbm.a.35326>.
- Cardoso, A.K.M.V., De Almeida Barbosa, A., Borges Miguel, F., Marcantonio, E., Farina, M., De Almeida Soares, G.D., Paim Rosa, F., 2007. Histomorphometric analysis of tissue responses to bioactive glass implants in critical defects in rat calvaria. *Cells Tissues Organs* 184, 128–137. <https://doi.org/10.1159/000099619>.
- Carrow, J.K., Cross, L.M., Reese, R.W., Jaiswal, M.K., Gregory, C. A., Kaunas, R., Singh, I., Gaharwar, A.K., 2018. Widespread changes in transcriptome profile of human mesenchymal stem cells induced by two-dimensional nanosilicates. *Proc. Natl. Acad. Sci. U. S. A.* 115, E3905–E3913. <https://doi.org/10.1073/pnas.1716164115>.
- Ducheyne, P., Qiu, Q., 1999. Bioactive ceramics: the effect of surface reactivity on bone formation and bone cell function. *Biomaterials* 20, 2287–2303. [https://doi.org/10.1016/S0142-9612\(99\)00181-7](https://doi.org/10.1016/S0142-9612(99)00181-7).
- El-Ghannam, A., 2005. Bone reconstruction: from bioceramics to tissue engineering. *Expert Rev. Med. Devices* 2, 87–101. <https://doi.org/10.1586/17434440.2.1.87>.
- El-Ghannam, A., Ducheyne, P., Shapiro, I.M., 1999. Effect of serum proteins on osteoblast adhesion to surface-modified bioactive glass and hydroxyapatite. *J. Orthop. Res.* 17, 340–345. <https://doi.org/10.1002/jor.1100170307>.
- El-Ghannam, A., Ning, C.Q., 2006. Effect of bioactive ceramic dissolution on the mechanism of bone mineralization and guided tissue growth in vitro. *J. Biomed. Mater. Res. - Part A* 76, 386–397. <https://doi.org/10.1002/jbm.a.30517>.
- El-Rashidy, A.A., Roether, J.A., Harhaus, L., Kneser, U., Boccaccini, A.R., 2017. Regenerating bone with bioactive glass scaffolds: a review of in vivo studies in bone defect models. *Acta Biomater.* <https://doi.org/10.1016/j.actbio.2017.08.030>.
- Gupta, G., Kirakodu, S., El-Ghannam, A., 2010. Effects of exogenous phosphorus and silicon on osteoblast differentiation at the interface with bioactive ceramics. *J. Biomed. Mater. Res. - Part A* 95, 882–890. <https://doi.org/10.1002/jbm.a.32915>.
- Gupta, G., Kirakodu, S., El-Ghannam, A., 2007. Dissolution kinetics of a Si-rich nanocomposite and its effect on osteoblast gene expression. *J. Biomed. Mater. Res. Part A* 80A, 486–496. <https://doi.org/10.1002/jbm.a.31005>.
- Han, P., Wu, C., Xiao, Y., 2013. The effect of silicate ions on proliferation, osteogenic differentiation and cell signalling pathways (WNT and SHH) of bone marrow stromal cells. *Biomater. Sci.* 1, 379–392. <https://doi.org/10.1039/c2bm00108j>.
- Liu, X., El-Ghannam, A., 2010. Effect of processing parameters on the microstructure and mechanical behavior of silica-calcium phosphate nanocomposite. *J. Mater. Sci. Mater. Med.* 21, 2087–2094. <https://doi.org/10.1007/s10856-010-4062-0>.
- Livak, K.J., Schmittgen, T.D., 2001. Analysis of relative gene expression data using real-time quantitative PCR and the 2- $\Delta\Delta$ CT method. *Methods* 25, 402–408. <https://doi.org/10.1006/meth.2001.1262>.
- Maniatopoulos, C., Sodek, J., Melcher, A.H., 1988. Bone formation in vitro by stromal cells obtained from bone marrow of young adult rats. *Cell Tissue Res.* 254, 317–330. <https://doi.org/10.1007/BF00225804>.
- Mao, L., Xia, L., Chang, J., Liu, J., Jiang, L., Wu, C., Fang, B., 2017. The synergistic effects of Sr and Si bioactive ions on osteogenesis, osteoclastogenesis and angiogenesis for osteoporotic bone regeneration. *Acta Biomater.* 61, 217–232. <https://doi.org/10.1016/j.actbio.2017.08.015>.
- Meijer, G.J., De Bruijn, J.D., Koole, R., Van Blitterswijk, C.A., 2007. Cell-based bone tissue engineering. *PLoS Med.* 4, 0260–0264. <https://doi.org/10.1371/journal.pmed.0040009>.
- Merry, K., Dodds, R., Littlewood, A., Gowen, M., 1993. Expression of osteopontin mRNA by osteoclasts and osteoblasts in modelling adult human bone. *J. Cell Sci.* 104.
- Müller, P., Bulnheim, U., Diener, A., Lüthen, F., Teller, M., Klinkenberg, E.D., Neumann, H.G., Nebe, B., Liebold, A., Steinhoff, G., Rychly, J., 2008. Calcium phosphate surfaces promote osteogenic differentiation of mesenchymal stem cells. *J. Cell. Mol. Med.* 12, 281–291. <https://doi.org/10.1111/j.1582-4934.2007.00103.x>.
- Porter, A.E., Patel, N., Skepper, J.N., Best, S.M., Bonfield, W., 2004. Effect of sintered silicate-substituted hydroxyapatite on remodelling processes at the bone-implant interface. *Biomaterials* 25, 3303–3314. <https://doi.org/10.1016/j.biomaterials.2003.10.006>.
- Reffitt, D.M., Ogston, N., Jugdaohsingh, R., Cheung, H.F.J., Evans, B.A.J., Thompson, R.P.H., Powell, J.J., Hampson, G.N., 2003. Orthosilicic acid stimulates collagen type I synthesis and osteoblastic differentiation in human osteoblast-like cells in vitro. *Bone* 32, 127–135. [https://doi.org/10.1016/S8756-3282\(02\)00950-X](https://doi.org/10.1016/S8756-3282(02)00950-X).
- Rodrigues, W.C., Fabris, A.L.D.S., Hassumi, J.S., Gonçalves, A., Sonoda, C.K., Okamoto, R., 2016. Kinetics of gene expression of alkaline phosphatase during healing of alveolar bone in rats. *Br. J. Oral Maxillofac. Surg.* 54, 531–535. <https://doi.org/10.1016/j.bjoms.2016.02.018>.
- Shie, M.Y., Ding, S.J., Chang, H.C., 2011. The role of silicon in osteoblast-like cell proliferation and apoptosis. *Acta Biomater.* 7, 2604–2614. <https://doi.org/10.1016/j.actbio.2011.02.023>.
- Simonsen, J.L., Rosada, C., Serakinci, N., Justesen, J., Stenderup, K., Rattan, S.I.S., Jensen, T.G., Kassem, M., 2002. Telomerase expression extends the proliferative life-span and maintains the osteogenic potential of human bone marrow stromal cells. *Nat. Biotechnol.* 20, 592–596. <https://doi.org/10.1038/nbt0602-592>.
- Spicer, P.P., Kretlow, J.D., Young, S., Jansen, J.A., Kasper, F.K., Mikos, A.G., 2012. Evaluation of bone regeneration using the rat critical size calvarial defect. *Nat. Protoc.* 7, 1918–1929. <https://doi.org/10.1038/nprot.2012.113>.
- Stein, G.S., Lian, J.B., Van Wijnen, A.J., Stein, J.L., Montecino, M., Javed, A., Zaidi, S.K., Young, D.W., Choi, J.Y., Pockwinse, S.M., 2004. Runx2 control of organization, assembly and activity of the regulatory machinery for skeletal gene expression. *Oncogene.* <https://doi.org/10.1038/sj.onc.1207676>.
- Tang, D., Tare, R.S., Yang, L.Y., Williams, D.F., Ou, K.L., Oreffo, R. O.C., 2016. Biofabrication of bone tissue: approaches, challenges and translation for bone regeneration. *Biomaterials.* <https://doi.org/10.1016/j.biomaterials.2016.01.024>.
- Vajgel, A., Mardas, N., Farias, B.C., Petrie, A., Cimões, R., Donos, N., 2014. A systematic review on the critical size defect model. *Clin. Oral Implants Res.* 25, 879–893. <https://doi.org/10.1111/clr.12194>.
- Wan, D.C., Nacamuli, R.P., Longaker, M.T., 2006. Craniofacial bone tissue engineering. *Dent. Clin. North Am.* 50, 175–190. <https://doi.org/10.1016/j.chroma.2005.12.062>.
- Will, J., Gerhardt, L.C., Boccaccini, A.R., 2012. Bioactive glass-based scaffolds for bone tissue engineering. *Adv. Biochem. Eng. Biotechnol.* https://doi.org/10.1007/10_2011_106.